PKD promotes activity-dependent AMPA receptor endocytosis in hippocampal neurons

Carlos O. Oueslati Morales[1], Attila Ignácz[2], Norbert Bencsik[2], Anikó Erika Rátkai[2], Wolfgang S. Lieb[1], Stephan A. Eisler[1,3], Katalin Schlett[2], Angelika Hausser[1,3#]

1 Institute of Cell Biology and Immunology, University of Stuttgart, D-70569 Stuttgart, Germany
2 Department of Physiology and Neurobiology, Eötvös Loránd University, H-1117 Budapest, Hungary
3 Stuttgart Research Center Systems Biology, University of Stuttgart, D-70569 Stuttgart, Germany
Corresponding author: angelika.hausser@izi.uni-stuttgart.de

Abstract

AMPA type glutamate receptors (AMPARs) mediate the majority of fast excitatory neurotransmission in the brain. The continuous trafficking of AMPARs into and out of synapses is a core feature of synaptic plasticity, which is considered as the cellular basis of learning and memory. The molecular mechanisms underlying the postsynaptic AMPAR trafficking, however, are still not fully understood. In this work, we demonstrate that the Protein Kinase D (PKD) family promotes basal and activity-induced AMPAR endocytosis in primary hippocampal neurons. Pharmacological inhibition of PKD increased synaptic levels of GluA1-containing AMPARs and slowed down their endocytic trafficking. By contrast, ectopic expression of constitutive active PKD decreased the synaptic level of AMPARs, while increasing their co-localization with early endosomes. On a molecular level, we identify PKD-mediated phosphorylation of the Rab5 effector protein Rabaptin-5 to be required for promoting activity-dependent AMPAR endocytosis. Our results thus establish an important role for PKD in the regulation of postsynaptic AMPAR trafficking during synaptic plasticity.

Keywords

AMPA receptor, GluA1, PKD, endocytosis, chemically induced LTD, Rabaptin5

Introduction

Synaptic plasticity describes a process where synaptic strength is changed in an activity-dependent manner within the brain. The most widely investigated forms of long-term synaptic changes include long-term potentiation (LTP) or long-term depression (LTD), which constitute the cellular basis of learning and memory [1,2]. One of the key elements in the control of synaptic strength is the dynamic alteration in the number and composition of the ionotropic AMPA-type glutamate receptors (AMPARs) within the postsynaptic membrane [1-3].

AMPARs are tetramers composed of four different subunits, GluA1-GluA4. Binding of glutamate allows the opening of the ion channel and the subsequent influx of Na^+ (and potentially Ca^{2+}) and efflux of K^+, causing membrane depolarization. Thus, the main function of AMPARs is to mediate excitatory neurotransmission in the brain [3,4]. The heterotetramer GluA1/2 is the most abundant variant followed by GluA2/3, while the GluA4 subunit is expressed mainly during early development and is present only at low levels in the adult brain [5-7]. GluA1-containing AMPARs leave the ER rapidly and are trafficked towards the synaptic plasma membrane. Plasma membrane insertion is thought to happen mostly within the extra- or perisynaptic regions, followed by a lateral movement of AMPARs into the synapse. Within the synaptic membrane, AMPARs are stabilized by postsynaptic density (PSD) scaffolding proteins in an activity-dependent manner [7-10]. Mature AMPARs are constitutively recycled through endocytic trafficking pathways: AMPARs are internalized from the cell surface at so-called Endocytic Zones localized adjacent to the PSD. Subsequently, AMPARs are trafficked to early endosomes and either recycled back to the plasma membrane or transported to dendritic lysosomes and degraded [11-14]. During LTD and LTP, endocytotic and exocytotic AMPAR trafficking is imbalanced, resulting in reduced and enhanced numbers of AMPARs at the synapse, respectively [11,15-17].

The protein kinase D (PKD) family of serine/threonine kinases belongs to the calmodulin-dependent protein kinases (CaMKs) superfamily, and comprises three isoforms in mammals: PKD1, PKD2 and PKD3; all of which are expressed in neurons from a very early embryonic stage [18,19]. PKDs are recruited to the plasma membrane or to different organelles, such as the Golgi complex, by binding to diacylglycerol. Upon activation, they control different intracellular processes such as vesicle fission from the Golgi complex and rearrangement of the actin cytoskeleton [18,20-22]. In breast cancer cells, PKD-mediated phosphorylation of Rabaptin-5, a binding partner for both Rab4 and Rab5, is required to shunt integrin $\alpha_v\beta_3$ to the short recycling loop, indicating a role for the kinase in endocytic trafficking processes [23,24]. In neurons, PKD plays a key role in the establishment and maintenance of polarity through controlling the integrity of the Golgi complex and trans-Golgi network-derived (TGN) sorting of vesicles [25-27]. Furthermore, we recently demonstrated a role for PKD in learning and memory through stabilization of plasticity-induced actin rearrangements [28]. However, so far PKD has not been linked to AMPAR trafficking in neuronal cells.

Here, we identify PKD as a regulator of basal and activity-mediated GluA1 endocytosis in cultured hippocampal neurons. We provide evidence that PKD is activated downstream of chemically induced GluA1 endocytosis. Inhibition of PKD increases surface and synaptic levels of GluA1. We further show that expression of constitutive active PKD (caPKD) decreases the synaptic amount of GluA1 while increasing the localization of GluA1 at early endosomes. Importantly, PKD inhibition blocks the endocytosis of GluA1 upon chemically evoked LTD (cLTD). On a molecular level, we identify PKD-mediated phosphorylation of the Rab5 effector

protein Rabaptin-5 to be required for endocytosis of GluA1. Combined, our data identify a previously unknown role of the PKD family in the regulation of AMPAR endocytosis in cultured hippocampal neurons.

Material and methods

Animal handling

CD1 mice (Charles River) were kept in the animal facility of the Institute of Cell Biology and Immunology, University of Stuttgart; or of the Biological Institute, Eötvös Loránd University, at 22 ± 1°C with 12 h light and dark cycles and ad libitum access to water and food. The animals were maintained and handled in accordance with the Guidelines for Accommodation and Care of Animals, according to the European Convention for the Protection of Vertebrate Animals Used for Experimental and Other Scientific Purposes.

Cell culture

Primary cultures of embryonic hippocampal cells were obtained from CD1 mice on embryonic day E17-E18 according to a published protocol [27]. In brief, cells were plated on poly-L-lysine-coated (PLL, Sigma #5899) 6 well plates (Greiner Bio-One, #657160) or 35 mm petri dishes (Greiner Bio-One, #627160) at a density of 4 x 10^5 cells/well. For imaging, cells were seeded on PLL/laminin-coated (Sigma; #L2020) glass coverslips (Carl Roth, #YX03.1) in 24-well plates or on glass bottom petri-dishes (Greiner Bio-One, #627870) at a density of 1.15 x 10^5 cells/well. Five days after plating, half of the original NeuroBasal culture mediu (ThermoFisher Scientific, #21103049) supplemented with B27 (ThermoFisher Scientific, #17504044) was changed to Brainphys (Stemcell technologies, #05790) supplemented with SM1 (Stemcell technologies, #05711), gentamycin (Sigma, #G1397) and amphotericin B (Gibco, #15290-026), containing 10 µM cytosin-arabinofuranoside (Sigma, #C6645). The cells were cultivated for 13 days at 37°C in 5% CO_2, and one half of the Neurobasal media was exchanged by fresh supplemented Brainphys every 3 days. HEK293T cells were cultivated in RPMI medium (Gibco, #21875-034) supplemented with 10% fetal bovine serum (FBS, Pan Biotech, #P30-3309). Chemically-induced Long Term Depression (cLTD) was induced by treating the neuronal cultures with 50 µM NMDA (Sigma, #M3262) for 5 min in conditioned medium. Then, cells were changed to a NMDA-free medium, and incubated for 15 min before being further processed. Agonist-induced AMPAR endocytosis was performed by treating the neuronal cultures with 100 µM S-AMPA (Hello Bio, #HB0052) and 50 µM D-AP5 (Tocris #3693) for 2 minutes in conditioned medium. Afterwards, cells were changed to an AMPA- and D-AP5-free medium and incubated for 10 minutes before being further processed.

Chemical treatments, antibody feeding and cell surface biotinylation

PKD activity was blocked with CRT0066101 (CRT, Tocris #4975) [29] diluted in dimethyl sulfoxide (DMSO), at a final concentration of 2 µM. For surface biotinylation of endogenous GluA1, 13-day-old neuronal cultures were placed on ice (13 days in vitro; DIV13), washed twice with calcium- and magnesium-containing phosphate-buffered saline (PBSCM, ThermoFisher Scientific, #14040-091) and incubated with 1.5 mg/ml sulfo-NHS-SS-biotin (ThermoFisher Scientific, #21331) diluted in PBSCM for 15 min. Afterwards, cultures were washed twice with 20 mM glycine (Roth, #HN07.1) in PBSCM for 7 min, to bind free biotin; before being finally lysed. To visualize surface GluA1, we employed an antibody feeding assay

modified from a published protocol [30]. In brief, neuronal cultures were incubated with an N-terminal-specific GluA1 antibody (1:100, Merck, #MAB2263) in conditioned media for 10 min at 37 °C and 5% CO_2 in a humidified atmosphere. Afterwards, cells were washed with PBS and fixed with 4% paraformaldehyde (PFA) in PBS for 10 min at room temperature (RT) without permeabilization. After 1 h of blocking with 5% FBS and 0.1% NaN_3 in PBS, a secondary anti-mouse antibody labelled with Alexa 546 (1:500, Invitrogen, #A11030) was applied to the cells for 1h at RT. Cells were washed and fixed again with 4% PFA in PBS for 10 min and further processed for Shank2 staining (see section Immunostaining and confocal laser scanning microscopy). Samples were mounted in ProLong Gold Antifade Mountant (ThermoFisher Scientific, #P36930) and analyzed by confocal laser scanning microscopy.

To analyze the amount of endocytosed AMPAR, biotinylation assays of receptor internalization were employed as described [11]. In brief, protein lysosomal degradation was inhibited with 100 µg/ml Leupeptin (Tocris, #1167) for 1h; then cells were placed on ice and incubated with 1.5 mg/ml Sulfo-NHS-SS-biotin (ThermoFisher Scientific, #21331) for 1 h. Subsequently, cells were transferred to biotin-free medium and treated with 100 µm S-AMPA and 50 µM D-AP5 for 2 min. Then, cells were returned to an AMPA- and D-AP5 free medium for 10 min to allow for endocytosis, subsequently placed again on ice and washed twice with cold PBSCM. Remaining surface biotin was cleaved by incubation with glutathione cleavage buffer (50 nM L-Glutathione (Sigma #G6013, 75 mM NaCl, 10 mM EDTA, 1% BSA, pH 8.6) for 15 min. Finally, cells were washed twice and further processed for protein extraction.

Protein extraction, biotin pulldowns and Western Blotting

Neuronal cells were harvested in cold lysis buffer (1% Triton X-100, 20 mM Tris pH 7.5, 150 mM NaCl, 1mM EDTA, 1 mM EGTA; 4°C) supplemented with protease (Roche, #11697498001) and phosphatase inhibitors (Roche, #04906845001), and subsequently centrifugated at 13000 x g for 10 min. For the biotin pulldowns, equal amounts of cell lysate were incubated with avidin-coated agarose beads (Thermo Scientific, #29201) for 90 min at 4°C and washed 4 times with lysis buffer. HEK293T cells were harvested in homogenization buffer (300 mM NaCl, 10 mM $MgCl_2$, 10% glycerol, 20 mM HEPES, 0.1% NP-40 and 1 mM DTT) supplemented with protease and phosphatase inhibitors, and subsequently centrifuged at 9300G for 3 min. To determine Rab5 activity, equal amounts of cell lysate were incubated with GST-tagged Rabaptin-5:Rab5 Binding Domain beads [31] for 60 min at 4°C and then washed once with homogenization buffer. Equal amounts of protein were run on NuPage Novex 4-12% Bis-Tris gels (Thermo Fisher Scientific, #NP0322BOX) and blotted onto nitrocellulose membranes using the iBlot device (Thermofisher scientific, #IB1001). Membranes were blocked for 30 min with 0.5% (v/v) blocking reagent (Roche, #11096176001) in PBS containing 0.05% Tween 20 and 0.1% NaN_3, and subsequently incubated with primary antibodies overnight at 4°C (anti-PKD1 (1:1000, Cell Signaling Technologies, CST, #2052), anti-pS916PKD (1:1000, CST, #2051), anti-actin (1:1000, Sigma, #A4700), anti-GluA1 (1:1000, Merck, #MAB2263), anti-pS831GluA1 (1:1000, CST, #75574), anti-GFP (1:2000, Roche, #11814460001)). The next day, membranes were washed and incubated with HRP-conjugated secondary anti-mouse and anti-rabbit antibodies at RT for 1 h (1:10000, Dianova, #115-035-062 or #111-035-144) before being washed again and finally visualized using the SuperSignal West Pico PLUS or the SuperSignal West Dura Extended Duration substrates (Thermo Fisher Scientific, #34580 or #34076). Proteins were visualized using the Amersham Imager 600, an enhanced chemiluminescence detection system (Thermo Fisher Scientific, Waltham, MA, USA). Quantitative Western Blotting chemiluminescence was detected at a

depth of 16-bit in the linear detection range of the device, equipped with a 3.2-megapixel super-honeycomb CCD camera fitted with a large aperture f/0.85 FUJINON lens. Special care was taken not to overexpose in order to guarantee accurate quantifications. For all proteins, at least three independent membranes were analyzed. Densitometry was performed using Image Studio Lite 5.2 (Li-COR Biosciences, Bad Homburg, Germany). For each protein, the integrated density of the signal was measured, corrected for background signals and adjusted to loading controls.

Transfection and expression constructs

On DIV12, neuronal cultures were transfected using Lipofectamine 2000 (Invitrogen, #11668-019) according to the manufacturer´s instructions. In brief, 0.5 µg of plasmid DNA was mixed with Lipofectamine 2000 in a 1 µg: 2 µl ratio. Medium was changed 4 h after transfection to the original cultivation medium and cells were incubated overnight. For transient transfections of HEK293T cells, TransIT293 reagent (Mirus, #2700) was used according to the manufacturer´s instructions. The enhanced green fluorescent protein (EGFP) vector was obtained from Clontech Europe, whereas the pcDNA3-mRuby2 was a gift from Michael Lin (Addgene plasmid #40260; http://n2t.net/addgene:40260; RRID:Addgene_40260) and pCI-SEP-GluR1 was a gift from Robert Malinow (Addgene plasmid #24000; http://n2t.net/addgene:24000; RRID:Addgene_24000) [32]. EGFP-Rabaptin-5 [33] wild type and EGFP-Rabaptin-5 S407A [24] were kindly provided by Alex Toker, Beth Israel Deaconess Center, Harvard Medical School, USA. caPKD1-EGFP has already been described elsewhere [34]. The GFP-Rabex-5 plasmid [35] was a generous gift from Juan Bonifacino, Division of Intramural Research, NICHD, USA while the pGEX-4 T-2/Rabaptin-5:R5BD was acquired from the lab of Guangpu Li, Fujian Agriculture & Forestry University, China [36]. The GFP-Rab5 wild type was received from Lucas Pelkmans, Institute of Molecular Life Sciences, University of Zurich, Switzerland [37].

Immunostaining and confocal laser scanning microscopy

Hippocampal cultures were fixed on DIV13 for 10 min with 4% PFA in PBS. After washing with PBS, cells were permeabilized with 0.1% Triton X-100 in PBS for 5 min. Cells were again washed with PBS and blocked with 5% FBS and 0.1% NaN_3 in PBS for 1 h at RT. Subsequently, the corresponding primary antibody (anti-Shank2 (1:2000, Synaptic Systems, #162204), anti-GluA1 (1:500, Merck, #MAB2263), anti-EEA1 (1:100, CST, #3288)) was diluted in blocking buffer and incubated for 1.5 h at RT. Cells were washed with PBS, and Alexa-Fluor-(546 or 633) labelled secondary antibodies (ThermoFisher Scientific #A-11030 and #A-21052, respectively) were diluted 1:500 in blocking buffer and incubated for 1 h at RT. Finally, samples were mounted in ProLong Gold Antifade. All samples were imaged using a confocal laser scanning microscope (LSM 710, Carl Zeiss) equipped with either a Plan Apochromat 63x/1.40 DIC M27 or an alpha Plan-Apochromat 100x/1.46 Oil DIC objective (Carl Zeiss), using sequential excitation with an 488 nm Argon laser, an 561 DPSS laser or an 633 nm HeNe laser. Image acquisition for the quantitative measurement of GluA1 intensity was done as follows: z-stacks of 0.32 µm intervals were acquired throughout the selected neuronal branches of at least 20 nm in length. Image processing and analysis was performed with either ZEN blue (Carl Zeiss) or with ImageJ. Regions of interests (ROIs) were selected according to clear Shank2 immunopositivity at the plasma membrane along the shaft or within dendritic spines. Mean pixel intensity values of the GluA1 channel within the selected ROIs were measured, background corrected and normalized to the staining intensity in the control condition. In order

to analyze the co-localization between GluA1 and EEA1 signals, single images of selected neuronal branches were acquired. In all experiments, laser power was set so that there would be no saturation and maintained constant throughout the analyses of different samples from the same experiment. Image processing and analysis was performed with ZEN blue (Carl Zeiss) and ImageJ. The Mander's overlap coefficient of GluA1 with EEA1 was calculated and used as a measure of co-localization.

Fluorescence recovery after photobleaching (FRAP)

To investigate AMPAR trafficking to and from the plasma membrane, neuronal cultures were transfected with the super ecliptic pHluorin-tagged GluA1 (SEP-GluA1) and mRuby2 plasmids in a 5:3 ratio, and incubated overnight. On the next day, culture medium was changed to pre-heated live cell imaging buffer containing 142 mM NaCl, 5.4 Mm KCl, 1.8 mM $CaCl_2$, 1 mM NaH_2PO_4, 0.8 mM $MgSO_4$, 5 mM glucose and 25 mM HEPES with a pH of 7.4. The diffusion mobility of the GluA1-containing AMPARs was analyzed at 37°C and 5% CO_2 on a Zeiss Axio Observer Spinning Disc Microscope, using an alpha Plan-Apochromat 100x/1.46 Oil DIC objective and a Photometrix Evolve 512 EMCCD camera for image acquisition. Photobleaching was executed with a UGA-42 firefly photomanipulation system equipped with a 100 mW 473 nm laser (Rapp OptoElectronic, Germany). Cells were initially treated with 2 µM of CRT for 10 min, then selected dendritic spines were bleached with a high-intensity laser light (473 nm line, 10% laser power). Fluorescence intensity in the bleached areas was measured over time both before and after the bleaching event, taking images every 30 seconds for approx. 25 min. Intensity values were corrected with the background intensity values and normalized to the unbleached region. Fitting of the curves was performed with a one-phase exponential equation (Y=Y0 + (Plateau-Y0)*(1-exp(-K*x)); Prism 8, GraphPad Software, La Jolla, CA).

Statistical analysis of the data

For statistical evaluation, unpaired Student´s t test, multiple Student´s t tests, Mann-Whitney and Kruskal-Wallis tests were used employing GraphPad Prism 8 software. Data are displayed as mean ± SEM, mean ± 95% confidence interval (CI) or Tukey's box-and-whiskers plots.

Results

AMPAR basal trafficking is regulated by PKD

AMPAR surface expression and recycling are highly dynamic, with a half-time in the range of minutes [7]. To address the role of PKD in basal AMPAR trafficking, we thus subjected hippocampal neurons to an acute, short-term PKD inhibition (10 min) using CRT0066101 (referred to as CRT), a selective pan-inhibitor of all PKD isoforms [29]. In order to prove that this short-term treatment with CRT effectively inhibits PKD activity, we analyzed autophosphorylation of PKD at serine 916 (pS916PKD) as an indicator of kinase activity [38] along with the total levels of PKD (Figure 1a). In line with our previous results [27], we show that endogenous PKD is active in cultured hippocampal neurons under basal conditions. We further detect a strong and significant decrease in the relative level of pS916PKD in CRT treated cells compared to the DMSO treated control (Figure 1a, b), confirming the efficacy of the inhibitor under these conditions.

Next, to assess the surface expression of GluA1-containing AMPARs in hippocampal neurons treated with CRT or the solvent DMSO, we utilized cell surface protein tagging using sulfo-NHS-SS-biotin. After cell lysis, biotinylated proteins were precipitated and the total expression and surface levels of GluA1 were detected by Western Blot analysis (Figure 1c). Our data clearly indicate that already a short-term PKD inhibition significantly increased the relative amount of surface GluA1 compared to the DMSO treatment (Figure 1d).

Under basal conditions, AMPARs have a high turnover within spines [39,40] and are internalized in the vicinity of synapses [41]. To investigate whether short-term PKD inhibition affects the amount of GluA1 within the synapses, an antibody feeding assay was performed. Firstly, hippocampal cultures were treated with CRT or DMSO, and subsequently incubated with an antibody detecting the extracellular N-terminal domain of GluA1. Cells were then fixed and stained without permeabilization for the surface-bound N-terminal specific α-GluA1 antibody, followed by a subsequent permeabilization and immunostaining for Shank2, a marker of the PSD [42] (Figure 1e). Notably, our analysis reveals that inhibition of PKD significantly increased GluA1 intensity within Shank2-positive areas compared to the control (Figure 1f). Vice versa, transfection of hippocampal cells with a plasmid encoding a constitutively active S738/742E mutant form of PKD (caPKD-EGFP) significantly decreased the amount of GluA1 in Shank2 positive areas compared to cells transfected with EGFP as control (Figure 1 g, h). Hence, our data provide compelling evidence that PKD activity regulates the amount and PSD localization of GluA1-containing AMPARs in synapses under basal conditions.

PKD controls basal AMPAR endocytosis

To further investigate how PKD controls AMPAR trafficking, we measured fluorescence recovery after photobleaching (FRAP) of Super Ecliptic pHluorin (SEP)-tagged GluA1. SEP emits fluorescence under neutral pH conditions, allowing for the study of specific subpopulations of the tagged protein at the cell surface in relation to those fluorochromes which are internalized within vesicles [32]. Cultures were co-transfected with mRuby2 to visualize transfected neuronal cells. Neurons were treated with either CRT or DMSO for 10 min, then the fluorescent signal within the dendritic spines of imaged dendritic branches was bleached

and the recovery of the fluorescence intensity was measured for another 10 min (Figure 2a, b). To calculate the half-life and the mobile fraction of SEP-GluA1, we additionally fitted the recovery curves with a one-phase exponential equation (Figure 2c). In DMSO treated neurons, photobleaching of spine SEP fluorescence to background levels (Figure 2a, b) was followed by a fast recovery ($t_{½}$ = 14.52 seconds with 95% Cl of + 15.08 CI, Figure 2d) to 61.16% with a 95% CI of ± 3.4 of the original SEP-GluA1 intensity after 183 seconds (Figure 2e). Upon PKD inhibition, GluA1-SEP signal within the spines recovered significantly slower ($t_{½}$ = 114.47 seconds with 95% Cl of 77.67 and 38.26, Figure 2d), albeit to the same level as the control (Fig. 2b, c). Consequently, the mobile fraction of GluA1-SEP did not significantly change between the CRT and DMSO treated cultures (Figure 2e). These results suggest that PKD inhibition slows down the trafficking of cell surface SEP-GluA1.

It is well established that constitutive endocytosis at perisynaptic zones regulates the number of AMPARs at the postsynaptic level [14,43,11,41]. Furthermore, under basal conditions, AMPARs undergo a robust time-dependent endocytosis [11]. To clarify whether PKD is involved in basal AMPAR endocytosis, we firstly investigated whether PKD short-term inhibition affects basal trafficking of AMPARs to early endosomes. To that end, neuronal cells expressing caPKD-EGFP were treated with CRT or DMSO, fixed, permeabilized and stained for GluA1 and EEA1, a marker of early endosomes [44]. EGFP expressing neurons served as a control. EEA1 and GluA1 were present on dot-like structures distributed all over the dendritic branch (Figure 2f). This is in line with earlier reports showing that EEA1 participates in the endocytosis of AMPARs and is highly expressed in the postsynaptic compartment of hippocampal synapses [45,46]. To assess whether the amount of GluA1 at early endosomes changes upon increased PKD activity, we analyzed the co-localization of GluA1 and EEA1 by analyzing the Mander´s coefficient (Figure 2g). Our data show that the expression of caPKD significantly enhances the amount of GluA1 at early endosomes compared to the control. This was rescued back to the control level when cells were treated with CRT for 10 minutes prior to fixation (Figure 2g). Our results thus indicate that enhanced PKD activity promotes AMPAR endocytosis.

To corroborate this finding, we studied the phosphorylation of GluA1 at S831 and S845 in dependence of PKD activity. S831 phosphorylation is mediated by CaMKII and Protein Kinase C (PKC), promoting the targeting of GluA1 to the PSD and increasing single channel conductance [47-49] whereas phosphorylation of S845 is mediated by PKA, leading to an increased single-channel open probability and to targeting or retention of GluA1 at the cell surface [50,51,4]. Cells were treated with CRT or DMSO for 10 min, lysed and both the total and phosphorylated levels of GluA1 were measured via Western Blot (Figure 2h and j). Remarkably, while short-term inhibition of PKD did not modify basal pS845 GluA1 levels compared to the control (Figure 2i), our data show a significant increase of basal pS831GluA1 in CRT-treated cells when compared to the control (Figure 2k). These observations are in line with our previous results showing enhanced GluA1 levels at the PSD and slowed down GluA1 cell surface trafficking upon PKD inhibition. As S831-phosphorylated GluA1 subunits are enriched at the PSD [49], it further suggests that the occurrence of GluA1-containing AMPARs at the PSD is enhanced in PKD-inhibited cells.

Collectively, our data show that the basal endocytic trafficking of GluA1-containing AMPARs requires PKD activity.

PKD regulates activity-mediated AMPAR endocytosis

Given that PKD activity promotes basal endocytotic AMPAR trafficking, we next investigated whether the kinase also plays a role in agonist-induced AMPAR endocytosis from synapses. To do so, we employed the biotinylation assay of receptor endocytosis using sulfo-NHS-SS-biotin [11]. Briefly, biotinylated hippocampal cultures were treated with CRT or DMSO, followed by 2 minutes of 100 µM AMPA-evoked stimulation of AMPARs with simultaneously blocking NMDA receptors with 50 µM D-AP5 (see Figure S1a; treatment is designated as "AMPA"). Cells were incubated additionally for 10 min to allow for endocytosis before the remaining cell surface biotin was cleaved and cells were processed for analysis. In this way, GluA1 subunits remain biotinylated only within endosomes. In line with previous results, AMPA treatment induced GluA1 endocytosis as indicated by increased levels of endocytosed GluA1 in comparison to total GluA1 (126% ± 0.08 SEM compared to the control, Figure S1b, c). Strikingly, ligand-induced endocytosis of AMPARs was completely rescued when cells were pre-treated with CRT (72% ± 0.13 SEM compared to the control, Figure S1b, c). Notably, AMPA treatment also enhanced autophosphorylation of PKD, indicating that the kinase is a downstream target of AMPAR signalling. The AMPA-induced increase in kinase activity was completely blocked by pre-treatment of cells with CRT (Figure S1d, e).

Treatment of hippocampal neuronal cultures with NMDA promotes activity-dependent endocytosis of AMPARs thereby evoking LTD (designated as cLTD) [52-56]. In order to investigate whether PKD activity is specifically required for LTD induction, cells were treated with CRT or DMSO for 10 min followed by cLTD treatment for additional 5 min. Cells were then changed to an NMDA-free medium and incubated for 15 min to allow for receptor endocytosis before undergoing surface protein biotinylation using sulfo-NHS-SS-biotin (Figure 3a). After cell lysis, biotinylated proteins were precipitated and the total expression and surface levels of GluA1 were detected through Western Blot analysis (Figure 3b). Remarkably, cLTD treatment promoted a significant decrease in surface GluA1 (78% ± 0.01 SEM compared to the control) which could be rescued with CRT (124% ± 0.1 SEM compared to the control, Figure 3c). Our data also show an enhanced PKD phosphorylation upon cLTD treatment indicating that PKD is activated downstream of NMDA receptors. In line with our previous data (Figure 1), CRT treatment completely prevented NMDA-induced PKD activation (Figure 3d, e). GluA1 dephosphorylation at S845 is a prerequisite for the LTD-induced endocytosis of AMPARs [52,57,4]. In line with the literature, cLTD treatment promoted a significant decrease in the level of pS845 GluA1 compared to the control. Notably, the NMDA-induced dephosphorylation of S845 was not blocked with CRT treatment (Figure 3f, g) suggesting that PKD acts further downstream.

Collectively, our data demonstrate that PKD activity is required for the endocytosis of AMPARs during basal and activity-dependent trafficking.

PKD-mediated phosphorylation of Rabaptin-5 is required for Rab5 activation and activity-mediated AMPAR endocytosis

The small GTPase Rab5 regulates the fusion kinetics of plasma-derived endocytic vesicles with early endosomes in both basal and activity-mediated trafficking of AMPARs [58,59,30,60]. Rabaptin-5 forms a complex with Rabex-5, a Rab5-guanosine exchange factor (GEF), and Rab5, thereby promoting Rab5 activation during endocytosis [61,62]. Notably, Rabaptin-5 is a

PKD substrate implicated in the regulation of integrin receptor trafficking in cancer cells [24]. Therefore, we investigated whether PKD-mediated phosphorylation of Rabaptin-5 is required for Rab5 activity. To this end, we performed an effector pulldown assay using HEK293T cells transiently transfected with plasmids encoding EGFP-Rab5 (Rab5) in combination with either EGFP as a control or EGFP-Rabex-5 (Rabex-5) together with EGFP-Rabaptin-5 wild type (Rabaptin-5 wt) or EGFP-Rabaptin-5 S407A (Rabaptin-5 S/A; Figure S1 f, g). In the latter case, the PKD-specific phosphorylation site of Rabaptin-5 has been exchanged for an alanine, preventing upstream phosphorylation. In line with other reports [63,61,62], we detected an increased level of active Rab5 in cells expressing Rabaptin-5 wt compared to the control cells. By contrast, the phosphodeficient Rabaptin-5 S407A mutant was not able to promote Rab5 activity when compared to control cells (Figure S1 f, g). These results demonstrate that PKD mediated phosphorylation of Rabaptin-5 at S407 promotes activation of Rab5.

Additionally, we explored whether PKD-mediated phosphorylation of Rabaptin-5 is required to promote synaptic removal of AMPARs upon NMDA-induced LTD. We again employed the GluA1 antibody-feeding assay on hippocampal cultures transfected with plasmids encoding EGFP, Rabaptin-5 wt or Rabaptin-5 S407A and induced cLTD (Figure 4 a, b). When analyzing GluA1 intensity in Shank2 positive areas of untreated cells, we observed a significant increase in the Rabaptin-5 S407A expressing cells in comparison with the EGFP control. This, however, was not the case for the untreated Rabaptin-5 wt expressing cells and clearly indicates that expression of the phosphodeficient mutant of Rabaptin-5 increases synaptic GluA1 surface levels under basal conditions. Most importantly, cLTD treatment induced a significant decrease in GluA1 intensity within the synaptic areas both upon EGFP and Rabaptin-5 wt overexpression but not in Rabaptin-5 S407A expressing neurons (Figure 4a, b). Our data thus provide evidence that PKD activity regulates basal and activity-induced AMPAR endocytosis through phosphorylation of Rabaptin-5 at serine 407.

Discussion

In neurons, PKD regulates Golgi function and polarized secretory trafficking thereby contributing to dendrite development and the maintenance of neuronal polarity [64,27,65]. Moreover, PKD activity is required for memory formation and learning [28]. However, a role for PKD in the turnover of AMPARs has not been described yet. In the present study, we show that short-term inhibition of PKD activity increases the level of surface and synaptic GluA1-containing AMPARs under basal conditions and during chemically evoked AMPAR internalization. We further demonstrate that PKD is activated downstream of NMDA receptor and AMPAR stimulation and promotes AMPAR endocytosis process through phosphorylation of the Rab5 effector protein Rabaptin-5.

The dynamic regulation of the number of synaptic AMPARs is one of the main mechanisms modifying long-term synaptic efficacy. Our data highlight PKD as a novel member of the postsynaptic signaling machinery regulating activity-induced endocytosis of AMPARs. This is in line with our previous findings that PKD activity is required for the maintenance of the dendritic tree [27], as well as for the stabilization of the F-actin network within dendritic spines upon induction of LTP and learning and memory formation *in vivo* [28]. Accordingly, a dual role for PKD in synaptic plasticity becomes apparent: on the one hand, the kinase controls the activity-induced potentiation and enlargement of spines during cLTP [28], on the other hand it is required for the elimination of AMPARs from the cell surface during cLTD.

In line with our results, PKD has been already described to participate in endocytosis and recycling of membrane proteins in non-neuronal cells. In fibroblasts, PKD activity is necessary for PDGF-driven short-loop recycling of $\alpha_v\beta_3$ integrin [23]. However, in neurons, expression of dominant-negative kinase-dead PKD (kdPKD) was reported to increase the endocytosis rate of the TfR and LRP dendritic membrane proteins [26]. At first glimpse, these data seem to contradict our findings, however, the different experimental approaches used to block PKD activity (one day of kdPKD expression vs acute CRT-mediated inhibition) may account for the discrepancies observed. This is also underpinned by the fact that expression of kdPKD1 affected dendrite development and neuronal polarity [27] whereas we could not observe any morphological changes upon short-term PKD inhibition (data not shown). Furthermore, due to its established role in polarized secretory trafficking in neurons, long-term inhibition of PKD activity is expected to affect exocytotic trafficking as well [64]. Thus, the short-term chemical inhibition used in this study is more suitable to analyze PKD-dependent fast changes in endocytosis.

We further found that PKD regulates synaptic AMPAR surface expression through phosphorylation of its substrate, Rabaptin-5. Rabaptin-5 and the Rab5-GEF Rabex-5 function together to activate Rab5 and to promote the fusion of endocytotic vesicles with early endosomes [63,61,62]. Rab5 plays a critical role in the regulation of constitutive and activity-dependent AMPAR endocytosis [66,67] and is essential for LTD [66]. By investigating another potential downstream target of PKD, the Rab5-GEF RIN1, we recently showed that enhancing Rab5 activity is a critical step during activity-dependent AMPAR internalization [30]. In accordance, loss or inhibition of the Rab5 effector protein EEA1 results in increased GluA1-containing AMPAR surface expression [46,68] reminiscent of the increased GluA1 surface expression observed upon short-term PKD inhibition. Additionally, expression of constitutive active PKD enhanced the co-localization of GluA1 with EEA1 further supporting a role for PKD in promoting AMPAR endocytosis through Rabaptin-5 and Rab5.

Notably, Rabaptin-5 is also an effector of Rab4 [69], which regulates cargo recycling [70,71] and is also found on early endosomes [72,11]. In neurons, Rab4 regulates dendritic spine maintenance and constitutive AMPAR recycling from sorting endosomes [11,73,74]. Interestingly, Rab4 and Rabex-5 recruit Rabaptin-5 to early endosomes to subsequently activate Rab5 [75]. Additionally, in breast cancer cells, PKD-mediated Rabaptin-5 phosphorylation controls $\alpha_v\beta_3$ integrin recycling from early endosomes in a Rab4-dependent manner [23,24]. We thus propose that PKD-mediated phosphorylation of Rabaptin-5 promotes AMPAR endocytosis through coordinating its interaction with Rab4 and activation of Rab5. In support of this are the findings i) that Rabaptin-5 S407A cannot properly activate Rab5 (this study) and ii) that its ability to interact with Rab4 is markedly reduced [24].

The presence and regulation of post-translational modifications (PTMs) on neurotransmitter receptors modifies their function and trafficking and thus synaptic strength. PTMs have been described to mediate numerous processes including AMPAR membrane targeting, retention, conductance, endocytosis and degradation [47,76-84]. Several phosphorylation sites on GluA1 have already been shown to be important for stability at the PSD and AMPAR conductance [47,85,77,80], with S831 and S845 being best understood. CaMKII/PKC-mediated phosphorylation of S831 increases single-channel conductance [48,85]. Moreover, under basal conditions, pS831-GluA1 receptors are enriched at the PSD suggesting that phosphorylation at S831 increases GluA1 targeting to this compartment [49]. In agreement with this, we detected an increase in pS831 GluA1 levels upon short-term PKD inhibition, presumably as a consequence of impaired AMPAR endocytosis. PKA-mediated phosphorylation of S845 has been described to promote GluA1 targeting to the cell surface and single-channel open probability [50,51,82]. Notably, dephosphorylation at S845 is required for AMPAR endocytosis upon LTD [82]. Our data show that acute CRT treatment did not rescue the dephosphorylation of GluA1 at serine 845 in response to cLTD. This suggests that i) PKD activity promotes AMPAR endocytosis downstream of S845 dephosphorylation and ii) upon PKD inhibition, AMPARs are primed for their endocytosis but remain on the surface.

Based on our data we propose the following model on how PKD regulates AMPAR endocytic trafficking: under basal conditions, endogenous PKD is active and phosphorylates Rabaptin-5 thereby promoting its interaction with Rab4 on early endosomes and the activation of Rab5 through Rabex-5. Consequently, AMPARs are taken back from the synaptic membrane by Rab5-dependent endocytosis. Chemically-induced AMPAR endocytosis either through NMDA receptor or AMPAR stimulation further enhances PKD activity thus accelerating AMPAR elimination from the surface (Figure 4c).

As most excitatory transmission in the brain is mediated by the AMPARs, their dysfunction has been observed in many neuronal disorders, with Alzheimer disease (AD) being the best reported so far. High concentration of soluble oligomeric Aβ induces the removal of surface AMPARs at synapses, leading to synaptic depression and impaired synaptic plasticity and memory [86,87]. Strikingly, at preclinical stages of AD, the appearance of enlarged Rab5-positive early endosomes was associated with elevated Rab4 levels and Rabaptin-5 translocation to endosomes [88]. Indeed, hyperactivation of Rab5 has been observed in AD patients and mouse models of AD disease [89-91]. These data imply that endocytic uptake of AMPARs is enhanced in AD, however, whether this also correlates with increased PKD activity needs to be addressed in future studies.

Acknowledgments

We are grateful to Viktória Szentgyörgyi and Gisela Link (Institute for Cell Biology and Immunology, Germany) for their excellent technical assistance and Raluca Tamas (Institute for Cell Biology and Immunology, Germany) for critical reading of the manuscript.

Declarations

Funding

This study was funded by a grant from the German Research Foundation to AH (DFG HA-357/11-2), a travel exchange program funded by the DAAD (PPP Hungary 57215775 and 57392635), and by the National Brain Research Programs (KTIA_NAP_13-2-2014-0018 and 2017-1.2.1-NKP-2017-00002) to KS as well as the VEKOP-2.3.3-15-2016-00007 grant from NRDIO.

Conflicts of interest

All authors declare that they have no conflict of interest.

Ethical approval

All applicable international, national, and/or institutional guidelines for the care and use of animals were followed. This article does not contain any studies with human participants performed by any of the authors.

Authors' contributions

Conceptualization: Angelika Hausser, Katalin Schlett; Methodology: Carlos O. Oueslati Morales, Attila Ignacz, Norbert Bencsik, Aniko E. Ratkai, Wolfgang S. Lieb; Formal analysis and investigation: Carlos O. Oueslati Morales, Attila Ignacz, Aniko E. Ratkai, Norbert Bencsik, Stephan A. Eisler, Wolfgang S. Lieb; Writing - original draft preparation: Carlos O. Oueslati Morales; Writing - review and editing: Angelika Hausser, Katalin Schlett; Funding acquisition: Angelika Hausser, Katalin Schlett;

References

1. Malinow R et Malenka RC (2002) AMPA receptor trafficking and synaptic plasticity. Annual Reviews Neuroscience 25:103-129. doi:https://doi.org/10.1146/annurev.neuro.25.112701.142758
2. Huganir RL et Nicoll RA (2013) AMPARs and synaptic plasticity: the last 25 years. Neuron 80:704-717. doi:https://doi.org/10.1016/j.neuron.2013.10.025.
3. Chater TE et Goda Y (2014) The role of AMPA receptors in postsynaptic mechanisms of synaptic plasticity. Frontiers in cellular neuroscience 8:1-14. doi:https://doi.org/10.3389/fncel.2014.00401
4. Diering GH et Huganir RL (2018) The AMPA receptor code of synaptic plasticity. Cell 100:314-329. doi:https://doi.org/10.1016/j.neuron.2018.10.018
5. Zhu JJ Esteban JA, Hayashi Y et Malinow R (2000) Postnatal synaptic potentiation: delivery of GluR4-containing AMPA receptors by spontaneous activity. Nature Neuroscience 3:1098-1106. doi:https://doi.org/10.1038/80614
6. Lu W Shi Y, Jackson AC et al (2009) Subunit composition of synaptic AMPA receptors revealed by a single-cell genetic approach. Neuron 62:254-268. doi:https://doi.org/10.1016/j.neuron.2009.02.027
7. Henley JM et Wilkinson KA (2013) AMPA receptor trafficking and the mechanisms underlying synaptic plasticity and cognitive aging. Dialogues in Clinical Neuroscience 15:11-27
8. Greger IH Khatri L et Ziff EB (2002) RNA editing at Arg607 controls AMPA receptor exit from the endoplasmic reticulum. Neuron 34:759-772. doi:https://doi.org/10.1016/S0896-6273(02)00693-1
9. Makino H et Malinow R (2009) AMPA receptor incorporation into synapses during LTP: the role of lateral movement and exocytosis. Neuron 64:381-390. doi:https://doi.org/10.1016/j.neuron.2009.08.035
10. Pick JE et Ziff EB (2018) Regulation of AMPA receptor trafficking and exit from the endoplasmic reticulum. Molecular Cellular Neuroscience 91:3-9. doi:https://doi.org/10.1016/j.mcn.2018.03.004
11. Ehlers MD (2000) Reinsertion or degradation of AMPA receptors determined by activity-dependent endocytic sorting. Neuron 28:511-525. doi:https://doi.org/10.1016/s0896-6273(00)00129-x
12. Blanpied TA Scott DB et Ehlers MD (2002) Dynamics and regulation of clathrin coats at specialized endocytic zones of dendrites and spines. Neuron 36:435-449. doi:https://doi.org/10.1016/s0896-6273(02)00979-0
13. Van der Slujis P et Hoogenraad CC (2011) New insights in endosomal dynamics and AMPA receptor trafficking. Seminars in cell and developmental biology 22:499-505. doi:https://doi.org/10.1016/j.semcdb.2011.06.008
14. Lüscher C Xia H, Beattie EC et al (1999) Role of AMPA receptor cycling in synaptic transmission and plasticity. Neuron 24:649-658. doi:https://doi.org/10.1016/s0896-6273(00)81119-8
15. Carroll RC Lissin DV, von Zastrow M, Nicoll RA et Malenka RC (1999) Rapid redistribution of glutamate receptors contributes to long-term depression in hippocampal cultures. Nature neuroscience 2:454-460. doi:https://doi.org/10.1038/8123
16. Shi SH Hayashi Y, Petralia RS et al (1999) Rapid spine delivery and redistribution of AMPA receptors after synaptic NMDA receptor activation. Science 284:1811-1816. doi:https://doi.org/10.1126/science.284.5421.1811
17. Hayashi Y Shi SH, Esteban JA et al (2000) Driving AMPA receptors into synapses by LTP and CaMKII: requirement for GluR1 and PDZ domain interaction. Science 287:2262-2267. doi:https://doi.org/10.1126/science.287.5461.2262

18. Oster H Abraham D et Leitges M (2006) Expression of the protein kinase D (PKD) family during mouse embryogenesis. Gene expression patters 6:400-408. doi:https://doi.org/10.1016/j.modgep.2005.09.006
19. Ellwanger K Pfizenmaier K, Lutz S et Hausser A (2008) Expression patterns of protein kinase D 3 during mouse development. Biomed Central Developmental Biology 8. doi:https://doi.org/10.1186/1471-213x-8-47
20. Ellwanger K et Hausser A (2013) Physiological functions of Protein Kinase D *in vivo*. International union of biochemistry and molecular biology 65:98-107. doi:https://doi.org/10.1002/iub.1116
21. Olayioye MA Barisic S et Hausser A (2013) Multi-level control of actin dynamics by Protein Kinase D. Cell signalling 25:1739-1747. doi:https://doi.org/10.1016/j.cellsig.2013.04.010
22. Reinhardt R Truebestein L, Schmidt HA et Leonard TA (2020) It takes two to tango: activation of Protein Kinase D by dimerization. Bioessays. doi:https://doi.org/10.1002/bies.201900222
23. Woods AJ Dominic PW, Caswell PT et Normal JC (2004) PKD1/PKCmu promotes alpha-gamma-beta3 integrin recycling and delivery to nascent focal adhesions. The EMBO Journal 23:2531-2543. doi:https://doi.org/10.1038/sj.emboj.7600267
24. Christoforides C Rainero E, Brown KK, Normal JC et Toker A (2012) PKD controls avb3 integrin recycling and tumor cell invasive migration through its substrate Rabaptin-5. Developmental Cell 23:560-572. doi:https://doi.org/10.1016/j.devcel.2012.08.008
25. Yin DM Huang YH, Zhu YB et Wang Y (2008) Both the establishments and maintenance of neuronal polarity require the activity of protein kinase D in the Golgi apparatus. The journal of neuroscience 28:8832-8843. doi:https://doi.org/10.1523/jneurosci.1291-08.2008
26. Bisbal M Conde C, Donoso M et al (2008) Protein kinase D regulates trafficking of dendritic membrane proteins in developing neurons. Journal of neuroscience 28:9297-9308. doi:https://doi.org/10.1523/jneurosci.1879-08.2008
27. Czöndör K Ellwanger K, Fuchs YF et al (2009) Protein kinase D controls the integrity of Golgi apparatus and the maintenance of dendritic arborization in hippocampal neurons. Molecular biology of the cell 20:2108-2120. doi:https://doi.org/10.1091/mbc.e08-09-0957
28. Bencsik N Szíber Z, Lilliom H et al (2015) Protein Kinase D promotes plasticity-induced F--actin stabilization in dendritic spines and regulates memory formation. Journal of Cell Biology 210:771-783. doi:https://doi.org/10.1083/jcb.201501114
29. Harikumar K Kunnumakkara AB, Ochi N et al (2010) A novel small-molecule inhibitor of protein kinase D blocks pancreatic cancer growth *in vitro* and *in vivo*. Molecular Cancer Therapeutics 9:1136-1146. doi:https://doi.org/10.1158/1535-7163.mct-09-1145
30. Szíber Z Liliom H, Oueslati Morales CO et al (2016) Ras and rab interactor 1 control neuronal plasticity by coordinating dendritic filopodial motility and AMPA receptor turnover. Molecular biology of the cell 28:285-295. doi:https://doi.org/10.1091/mbc.e16-07-0526
31. Qi Y Liang Z, Wang Z et al (2015) Determination of Rab5 activity in the cell by effector pull-down assay. Methods molecular biology 1298:259-270. doi:https://doi.org/10.1007/978-1-4939-2569-8_22
32. Kopec CD Li B, Wei W, Boehm J et Malinow R (2006) Glutamate receptor exocytosis and spine enlargement during chemically induced long-term potentiation. The journal of neuroscience 26:2000-2009. doi:https://doi.org/10.1523/jneurosci.3918-05.2006
33. Mattera R Arighi CN, Lodge R, Zerial M et Bonifacio JS (2003) Divalent interaction of the GGAs with the Rabaptin-5-Rabex-5 complex. The EMBO Journal 22:78-88. doi:https://doi.org/10.1093/emboj/cdg015
34. Hausser A Link G, Bamberg L et al (2002) Structural requirements for localization and activation of protein kinase C mu at the Golgi compartment. The Journal of Cell Biology 156:65-74. doi:https://doi.org/10.1083/jcb.200110047

35. Mattera R Tsai YC, Weissman AM et Bonifacino JS (2006) The Rab5 guanine nucleotide exchange factor Rabex-5 binds ubiquitin and functions as a Ub ligase through an atypical Ub-interacting motif and a zinc finger domain. The journal of biological chemistry 281:6874-6883. doi:https://doi.org/10.1074/jbc.m509939200
36. Qi Y. Liang Z., Wang Z., et al (2015) Determination of Rab5 activity in the cell by effector pull-down assay. Methods molecular biology 1298:259-270. doi:https://doi.org/10.1007/978-1-4939-2569-8_22
37. Nagelkerken B Ankel Ev, Raak Mv et al (2000) Rabaptin4, a novel effector of the small GTPase rab4a, is recruited to perinuclear recycling vesicles. The Biochemical Journal 346:593-601
38. Matthews SA Rozengurt E et Cantrell D (1999) Characterization of serine 916 as an *in vivo* autophosphorylation site for protein kinase D/protein kinase Cmu. Journal of biological chemistry 274:26543-26549. doi:https://doi.org/10.1074/jbc.274.37.26543
39. Passafaro M Piëch V et Sheng M (2001) Subunit-specific temporal and spatial patterns of AMPA receptor exocytosis in hippocampal neurons. Nature neuroscience 4:917-926. doi:https://doi.org/10.1038/nn0901-917
40. Shi SH Hayashi Y, Esteban JA et Malinow R (2001) Subunit-specific Rules Governing AMPA Receptor Trafficking to Synapses in Hippocampal Pyramidal Neurons. Cell 105:331-343. doi:https://doi.org/10.1016/s0092-8674(01)00321-x
41. Rosendale M Jullié D, Choquet D et Perrais D (2017) Spatial and temporal regulation of receptor endocytosis in neuronal dendrites revealed by imaging of single vesicle formation. Cell Reports 18:1840-1847. doi:https://doi.org/10.1016/j.celrep.2017.01.081
42. Naisbitt S Kim E, Tu JC et al (1999) Shank, a novel family of postsynaptic density proteins that binds to the NMDA receptor/PSD-95/GKAP complex and cortactin. Neuron 23:569-582. doi:https://doi.org/10.1016/S0896-6273(00)80809-0
43. Man HY Lin JW, Ju WH et al (2000) Regulation of AMPA receptor-mediated synaptic transmission by clathrin-dependent receptor internalization. Neuron 25:649-662. doi:https://doi.org/10.1016/s0896-6273(00)81067-3
44. Mu FT Callaghan JM, Steele-Mortimer O et al (1995) EEA1, an early endosome associated protein. The journal of biological chemistry 270:13503-13511. doi:https://doi.org/10.1074/jbc.270.22.13503
45. Selak S Woodman RC et Fritzler J (2000) Autoantibodies to early endosome antigen (EEA1) produce a staining pattern resembling cytoplasmic anti-neutrophil cytoplasmic antibodies (C-ANCA). Clinical and experimental immunology 122:493-498. doi:https://doi.org/10.1046/j.1365-2249.2000.01390.x
46. Selak S Paternain AV, Fritzler MJ et Lerma J (2006) Human autoantibodies against early endosome antigen 1 enhance excitatory synaptic transmission. Neuroscience 143:953-964. doi:https://doi.org/10.1016/j.neuroscience.2006.10.014
47. Roche KW O´Brien RJ, Mammen AL, Bernhardt J et Huganir RL (1996) Characterization of multiple phosphorylation sites on the AMPA receptor GluR1 subunit. Neuron 16:1179-1188. doi:https://doi.org/10.1016/s0896-6273(00)80144-0
48. Barria A Derkach V et Sonderling T (1997) Identification of the ca2+/calmodulin-dependent protein kinase II regulatory phosphorylation site in the a-Amino-3-hydroxyl-5-methyl-4-isoxazole-propionate-type glutamate receptor. The journal of biological chemistry 272:32727-32730. doi:https://doi.org/10.1074/jbc.272.52.32727
49. Diering GH Heo S, Hussain NK, Liu B et Huganir RL (2016) Extensive phosphorylation of AMPA receptors in neurons. PNAS 113:4920-4927. doi:https://doi.org/10.1073/pnas.1610631113
50. Banke TG Bowie D, Lee H, Huganir RL, Schousboe A et Traynelis SF (2000) Control of GluR1 AMPA receptor function by cAMP-dependent protein kinase Journal of neuroscience 20:89-102. doi:https://doi.org/10.1523/jneurosci.20-01-00089.2000

51. Man HY Sekine-Aizawa Y et Huganir RL (2007) Regulation of alpha-amino-3-hydroxy-5-methyl-4-isoxazolepropionic acid receptor trafficking through PKA phosphorylation of the Glu receptor 1 subunit. Proc Natl Acad Sci USA 104:3579-3584. doi:https://doi.org/10.1073/pnas.0611698104
52. Lee HK Kameyama K, Huganir RL et Bear MF (1998) NMDA induces long-term synaptic depression and dephosphorylation of the GluR1 subunit of AMPA receptors in hippocampus. Neuron 21:1151-1162. doi:https://doi.org/10.1016/s0896-6273(00)80632-7
53. Beattie EC Carroll RC, Yu X et al (2000) Regulation of AMPA receptor endocytosis by a signaling mechanism shared with LTD. Nature 3:1291-1300. doi:https://doi.org/10.1038/81823
54. Lee SH Liu L, Wang YT et Sheng M (2002) Clathrin adaptor AP2 and NSF interact with overlapping sites of GluR2 and play distinct roles in AMPA receptor trafficking and hippocampal LTD. Neuron 36:661-674. doi:https://doi.org/10.1016/s0896-6273(02)01024-3
55. Lin DT et Huganir RL (2007) PICK1 and phosphorylation of the glutamate receptor 2 (GluR2) AMPA receptor subunit regulates GluR2 recycling after NMDA receptor-induced internalization. The journal of neuroscience 27:13903-13908. doi:https://doi.org/10.1016/s0896-6273(00)80632-7
56. Collingridge GL Peineau S, Howland JG et Wang YT (2010) Long-term depression in the CNS. Nature reviews neuroscience 11:459-473. doi:https://doi.org/10.1038/nrn2867
57. Lee HK Takamiya K, Han JS et al (2003) Phosphorylation of the AMPA receptor GluR1 subunit is required for synaptic plasticity and retention of spatial memory. Cell 112:631-643. doi:https://doi.org/10.1016/S0092-8674(03)00122-3
58. Gorvel JP Chavrier P, Zerial M et Gruenberg J (1991) Rab5 controls early endosome fusion in vivo. Cell 64:915-925. doi:https://doi.org/10.1016/0092-8674(91)90316-q
59. Bucci C Parton RG, Mather IH et al (1992) The small GTPase Rab5 functions as a regulatory factor in the early endocytic pathway. Cell 70:715-728. doi:https://doi.org/10.1016/0092-8674(92)90306-w
60. K Hausser A et Schlett (2017) Coordination of AMPA receptor trafficking by Rab GTPases. Small GTPases 0:1-14. doi:https://doi.org/10.1080/21541248.2017.1337546
61. Horiuchi H Lippé R, McBride HM et al (1997) A novel Rab5 GDP/GTP exchange factor complexed to Rabaptin-5 links nucleotide exchange to effector recruitment and function. Cell 90:1149-1159. doi:https://doi.org/10.1016/s0092-8674(00)80380-3
62. Zhang Z Zhang T, Wang S et al (2014) Molecular mechanism for Rabex-5 GEF activation by Rabaptin-5. eLife. doi:http://dx.doi.org/10.7554/eLife.02687
63. Stenmark H Vitale G, Ullrich O et Zerial M (1995) Rabaptin-5 is a direct effector of the small GTPase Rab5 in endocytic membrane fusion. Cell 83:423-432. doi:https://doi.org/10.1016/0092-8674(95)90120-5
64. Horton AC Rácz B, Monson EE; Lin AL, Weinberg RJ, Ehlers MD (2005) Polarized secretory trafficking directs cargo for assymetric dendrite growth and morphogenesis. Neuron 48:757-771. doi:https://doi.org/10.1016/j.neuron.2005.11.005
65. Quassollo G Wojnacki J, Salas DA et al (2015) A RhoA signaling pathway regulates dendritic Golgi outpost formation. Current biology 25:971-982. doi:https://doi.org/10.1016/j.cub.2015.01.075
66. Brown TC Tran IC, Backos DS et Esteban JA (2005) NMDA receptor-dependent activation of the small GTPase Rab5 drives the removal of synaptic AMPA receptors during hippocampal LTD. Neuron 45:81-94. doi:https://doi.org/10.1016/j.neuron.2004.12.023
67. Glebov OO Tigaret CM, Mellor JR et Henley JM (2014) Clathrin-independent trafficking of AMPARs. The journal of neuroscience 35:4830-4836. doi:https://doi.org/10.1523/jneurosci.3571-14.2015
68. Xu X et Pozzo-Miller L (2017) EEA1 restores homeostatic synaptic plasticity in hippocampal neurons from Rett syndrome mice. Journal of physiology 595:5699-5712. doi:https://doi.org/10.1113/jp274450

69. Vitale G Rybin V, Christoforidis S et al (1998) Distinct rab-binding domains mediate the interaction of rabaptin-5 with GTP-bound rab4 and rab5. EMBO Journal 17:1941-1951. doi:https://doi.org/10.1093/emboj/17.7.1941
70. Van der Slujis P Hull M, Webster P, Male P, Goud B et Mellman I (1992) The small GTP-binding protein rab4 control an early sorting event on the endocytic pathway. Cell 70:729-740. doi:https://doi.org/10.1016/0092-8674(92)90307-x
71. Wandinger-Ness A et Zerial M (2014) Rab proteins and the compartimentalization of the endosomal system. Cold Spring Harbor Perspective Biology 6. doi:https://doi.org/10.1101/cshperspect.a022616
72. Sönnichsen B Renzis S, Nielsen E, Rietdorf J et Zerial M (2000) Distinct membrane domains on endosomes in the recycling pathway visualized by multicolor imaging of rab4, rab5 and rab11. The Journal of Cell Biology 149:901-914. doi:https://doi.org/10.1083/jcb.149.4.901
73. Brown TC Correia SS, Petrok CN et Esteban JA (2007) Functional compartmentalization of endosomal trafficking for the synaptic delivery of AMPA receptors during long-term potentiation. The journal of neuroscience 27:13311-13315. doi:https://doi.org/10.1523/jneurosci.4258-07.2007
74. Gu Y Chiu S-L, Liu B et al (2016) Differential vesicular sorting of AMPA and GABAA receptors. Proc Natl Acad Sci USA 113:922-931. doi:https://doi.org/10.1073/pnas.1525726113
75. Kälin S Hirschmann DT, Buser DP et Spiess M (2015) Rabaptin5 is recruited to endosomes by rab4 and rabex5 to regulate endosome maturation. Journal of Cell Science 128:4126-4137. doi:https://doi.org/10.1242/jcs.174664
76. Chung HJ Xia J, Scannevin RH, Zhang X et Huganir RL (2000) Phosphorylation of the AMPA receptor subunit GluR2 differentially regulates its interaction with PDZ domain-containing proteins. Journal of neuroscience 20:7258-7267. doi:https://doi.org/10.1523/jneurosci.20-19-07258.2000
77. Esteban JA Shi SH, Wilson C, Nuriya M, Huganir RL et Malinow R (2003) PKA phosphorylation of AMPA receptor subunits controls synaptic trafficking underlying plasticity. Nature neuroscience 6:136-143. doi:https://doi.org/10.1038/nn997
78. Seidenman KJ Steinberg JP, Huganir R et Malinow R (2003) Glutamate receptor subunit 2 serine 880 phosphorylation modulates synaptic transmission and mediates plasticity in CA1 pyramidal cells. Journal of neuroscience 23:9220-9228. doi:https://doi.org/10.1523/jneurosci.23-27-09220.2003
79. Hayashi T et Huganir RL (2004) Tyrosine phosphorylation and regulation of the AMPA receptor by SRC family tyrosine kinases. Journal of neuroscience 24:6152-6160. doi:https://doi.org/10.1523/jneurosci.0799-04.2004
80. Boehm J Kang MG, Johnson RC, Esteban J, Huganir RL et Malinow R (2006) Synaptic incorporation of AMPA receptors during LTP is controlled by a PKC phosphorylation site on GluR1. Neuron 51:213-225. doi:https://doi.org/10.1016/j.neuron.2006.06.013
81. Steinberg JP Takamiya K, Shen Y et al (2006) Targeted in vivo mutations of the AMPA receptor subunit GluR2 and its interacting protein PICK 1 eliminate cerebellar long-term depression. Neuron 49:845-860. doi:https://doi.org/10.1016/j.neuron.2006.02.025
82. Lee HK Takamiya K, He K, Song L et Huganir RL (2010) Specific roles of AMPA receptor subunit GluR1 (GluA1) phosphorylation sites in regulating synaptic plasticity in the CA1 region of hippocampus. Journal of neurophysiology 103:479-489. doi:https://doi.org/10.1152/jn.00835.2009
83. Coultrap SJ Freund RK, O´Leary H et al (2014) Autonomous CaMKII mediates both LTP and LTD using a mechanism for differential substrate site selection. Cell Reports 6:431-437. doi:https://doi.org/10.1016/j.celrep.2014.01.005
84. Widagdo J Chai YJ, Ridder MC et al (2015) Activity-dependent ubiquitination of GluA1 and GluA2 regulates AMPA receptor intracellular sorting and degradation. Cell Reports 10:783-795. doi:https://doi.org/10.1016/j.celrep.2015.01.015

85. Derkach V Barria A et Soderling TR (1999) Ca2+/calmodulin-kinase II enhances channel conductance of a-amino-3-hydroxy-5-methyl-4-isoxazolepropionate type glutamate receptors. PNAS 96:3269-3274. doi:https://doi.org/10.1073/pnas.96.6.3269
86. Hsieh H Boehm J, Sato C et al (2006) AMPAR removal underlies ab-induced synaptic depression and dendritic spine loss. Neuron 52:831-843. doi:https://doi.org/10.1016/j.neuron.2006.10.035
87. Ganesh MS Bloodgood BL, Townsend M, Walsh DM, Selkoe DJ et Sabatini BL (2007) Natural oligomers of the Alzheimer amyloid-b protein induce reversible synapse loss by modulating an NMDA-type glutamate receptor-dependent signaling pathway. Journal of Neuroscience 27:2866-2875. doi:https://doi.org/10.1523/jneurosci.4970-06.2007
88. Cataldo AM Peterhoff CM, Troncoso JC, Gomez-Isla T, Hyman BT et Nixon RA (2000) Endocytic pathway abnormalities precede amyloid b deposition in sporadic Alzheimer´s disease and Down syndrome: differential effects of APOE genotype and presenilin mutations. The Americal Journal of Pathology 157:277-286. doi:https://doi.org/10.1016/s0002-9440(10)64538-5
89. Ginsberg SD Mufson EJ, Counts SE et al (2010) Regional selectivity of rab5 and rab7 protein up regulation in mild cognitive impairment and Alzheimer´s disease. Journal of Alzheimers Diseases 22. doi:https://doi.org/10.3233/jad-2010-101080
90. Ginsberg SD Alldred MJ, Counts SE et al (2010) Microarray analysis of hippocampal CA1 neurons implicates early endosomal dysfunction during Alzheimer´s disease progression. Biological Psychiatry 68:885-893. doi:https://doi.org/10.1016/j.biopsych.2010.05.030
91. Ginsberg SD Mufson EJ, Alldred MJ et al (2011) Upregulation of select rab GTPases in cholinergic basal forebrain neurons in mild cognitive impairment in Alzheimer´s diseases. Journal of chemical neuroanatomy 42:102-110. doi:https://doi.org/10.1016/j.jchemneu.2011.05.012

Figure legends

Fig. 1 PKD regulates basal AMPAR trafficking

Representative Western Blots obtained from hippocampal cultures treated with DMSO (-) or CRT displaying PKD and pS916PKD levels **(a)** and total and surface GluA1 levels upon biotinylation (**c**). Actin served as a loading control and is absent from the precipitated samples. **(b and d)** Quantification of data shown in (a) and (c), respectively, using densitometry analysis. Data from CRT-treated cultures are presented as mean line density ± SEM normalized to the control cultures; each dot represents one independent experiment. Statistical comparison was performed by unpaired two-tailed t-test. The dotted line indicates the control level. **(e and g)** Representative inverted single-channel and colored merged pictures of neuronal dendritic branches stained for the extracellular N-terminal domain of GluA1 and the PSD marker Shank2. Arrows point to Shank2-positive areas included in the analysis. The EGFP signal is not included in the colored merged image. **(f and h)** Quantification of pictures shown in (e) and (g), respectively. Data were normalized for the DMSO (f) or EGFP control (h). The boxplot shows the results of three independent experiments. Center lines show the medians; box limits indicate the 25th and 75th percentiles; whiskers extend 1.5 times the interquartile range from the 25th and 75th percentiles, outliers are represented by dots. The number of investigated sample points is N=171 and 273 (f) or N=220 and 223 (h), respectively. The significance of differences was analyzed by a Mann-Whitney test (two-tailed). *$p<0.05$, **$p<0.01$, ***$p<0.001$, ****$p<0.0001$. Scale bar 2 µm

Fig. 2 PKD specifically controls AMPAR endocytosis

(a) Representative pictures of neuronal dendritic spines expressing Super Ecliptic pHluorin-tagged GluA1 (SEP-GluA1) and mRuby2. Cells were treated with DMSO as a control or CRT prior to the bleaching event. Images show dendritic spines before bleaching, as well as 5, 60 and 600s afterwards. **(b)** Fluorescence recovery curve and **(c)** one-phase association curve fitting of the SEP-GluA1 intensity after bleaching. Data shown as mean ± SEM (b) or with 95% CI (c); n=3-4, N=14 and 27 analyzed cells, for DMSO and CRT-treated conditions, respectively. The significance of differences was analyzed by a multiple t-test, using the Holm-Sidak method. **(d)** Recovery half-time of the SEP-GluA1 signal and **(e)** mobile GluA1 fraction. Data shown as mean ± 95% CI. **(f)** Representative pictures of neuronal dendritic branches expressing EGFP or caPKD-EGFP. Cells were treated with DMSO (-) or CRT, fixed and stained for the early endosome marker EEA1 and for GluA1. Arrows point to the EEA1-positive early endosomes included in the analysis. The EGFP signal is not included in the colored merged image. **(g)** Manders´ overlap coefficient for EEA1 and GluA1. Quantification of pictures shown in (f). The boxplot shows the results of three independent experiments. Center lines show the medians; box limits indicate the 25th and 75th percentiles; whiskers extend 1.5 times the interquartile range from the 25th and 75th percentiles, outliers are represented by dots; N = 28 sample points each. The significance of differences was analyzed by a Kruskal-Wallis test with Dunn´s multiple correction. Representative Western Blot displaying total and pS845 GluA1 **(h)** as well as total and pS831 GluA1 **(j)** levels of DMSO (-) or CRT-treated hippocampal neuronal cultures. Actin served as a loading control. **(i and k)** Quantification of

data shown in (h) and (j), respectively, using densitometry analysis. Data are presented as mean line density ± SEM of CRT normalized to the control (-), each dot represents one independent experiment. Statistical comparison by unpaired two-tailed t-test. The dotted line indicates the control level. *p<0.05, **p<0.01. Scale bar 2 µm

Fig. 3 PKD activity is required for cLTD-induced AMPAR endocytosis

(a) Scheme displaying the cell surface biotinylation assay to detect the remaining surface GluA1 receptors after cLTD treatment. Cells were treated with DMSO or CRT followed by NMDA application. After the cLTD treatment, cultures were surface biotinylated using sulfo-NHS-SS-biotin and further processed. Representative Western Blots displaying **(b)** total and surface GluA1 levels, **(d)** PKD and pS916PKD levels, and **(f)** total and pS845GluA1 levels in biotinylated hippocampal neuronal cultures. Actin served as a loading control and is absent from the precipitated samples. **(c, e, g)** Quantification of data shown in (b,d, f), using densitometry analysis. Data are presented as mean line density ± SEM of treated samples (cLTD and cLTD plus CRT) normalized to the control; each dot represents one independent experiment. Statistical comparison was done by one-way ANOVA with Sidak´s correction. The dotted lines represent the control level.

Fig. 4 PKD-mediated phosphorylation of Rabaptin-5 is required for cLTD-induced AMPAR endocytosis

(a) Representative pictures of neuronal dendritic branches expressing EGFP, EGFP-tagged Rabaptin-5 wild-type (EGFP-Rabaptin-5 wt) or EGFP-tagged Rabaptin-5 S407A (EGFP-Rabaptin5 S/A) treated with sterile water (-) or NMDA. Cells were then stained for the extracellular domain of surface GluA1 and the PSD marker Shank2. Arrows point to Shank2-positive PSD areas included in the analysis. The EGFP signal is not included in the colored merged image. **(b)** Quantification of the images shown in (a). The boxplot shows the results of three independent experiments. Center lines show the medians; box limits indicate the 25th and 75th percentiles; whiskers extend 1.5 times the interquartile range from the 25th and 75th percentiles, outliers are represented by dots. N=769, 385, 835, 323, 661 and 331 sample points. The significance of differences was analyzed by a Kruskal-Wallis test with Dunn´s multiple correction. *p < 0.05, **p < 0.01, ****p < 0.0001. Scale bar 2 µm. **(c)** Proposed model of PKD signaling in endocytic AMPAR trafficking. For the explanation, see text.

Supplementary figure 1 PKD activity is required for agonist-induced AMPAR endocytosis and regulates Rab5 activity through Rabaptin-5 phosphorylation

(a) Scheme displaying the surface biotinylation assay for receptor internalization. After surface biotinylation, cells were treated with DMSO or CRT followed by AMPA and D-AP5 application. Afterwards, cultures were treated with glutathione to remove remaining surface biotin. Thereby, biotinylated GluA1 signal is detected only in endocytosed AMPARs, evoked by combined AMPA and D-AP5 treatment. Representative Western Blots displaying **(b)** total and internalized GluA1 levels and **(d)** PKD and pS916PKD levels in hippocampal neuronal cultures. Actin served as a loading control and is absent from the precipitated samples. **(c, e)**

Quantification of data shown in (b, d), using densitometry analysis. Data are presented as mean line density ± SEM of the treated samples (AMPA and AMPA plus CRT) normalized to the control, each dot represents one independent experiment. Statistical comparison was done by one-way ANOVA with Sidak´s correction. The dotted lines represent the control level. **(f)** Representative Western Blot displaying total and active Rab5 levels in HEK293T cells transiently transfected with plasmids encoding Rab5 and Rabex-5 in combination with either EGFP (-), Rabaptin-5 wt (wt) or Rabaptin-5 S407A (S/A). Active Rab5 was precipitated from the cell lysates using GST-tagged Rabaptin-5:Rab5 binding domain bound to glutathione sepharose beads. **(g)** Quantification of data shown in (f), using densitometry analysis. Data are presented as mean line density ± SEM of the Rabaptin-5 wt and S/A samples normalized to the control (EGFP), n=5. Statistical comparison by unpaired two-tailed t-test. *$p < 0.05$. The dotted line indicates the active Rab5 level of the EGFP control.

Figure 1

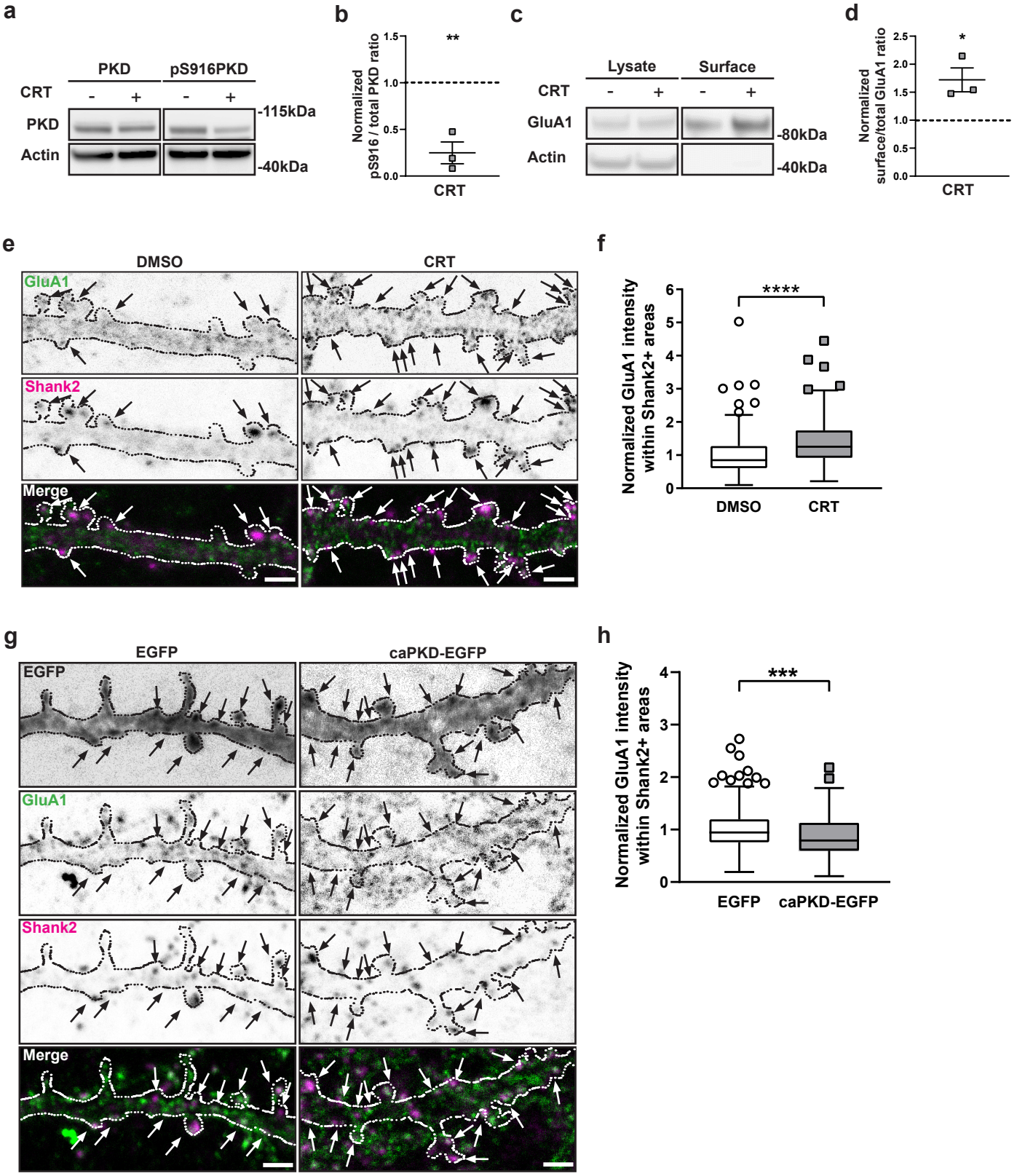
a
PKD
pS916PKD
CRT
-
+
-
+
PKD
Actin
-115kDa
-40kDa
b
Normalized pS916 / total PKD ratio
1.5
1.0
0.5
0.0
**
CRT
c
Lysate
Surface
CRT
-
+
-
+
GluA1
Actin
-80kDa
-40kDa
d
Normalized surface/total GluA1 ratio
2.5
2.0
1.5
1.0
0.5
0.0
*
CRT
e
DMSO
CRT
GluA1
Shank2
Merge
f
Normalized GluA1 intensity within Shank2+ areas
6
5
4
3
2
1
0
****
DMSO
CRT
g
EGFP
caPKD-EGFP
EGFP
GluA1
Shank2
Merge
h
Normalized GluA1 intensity within Shank2+ areas
4
3
2
1
0
***
EGFP
caPKD-EGFP

Figure 2

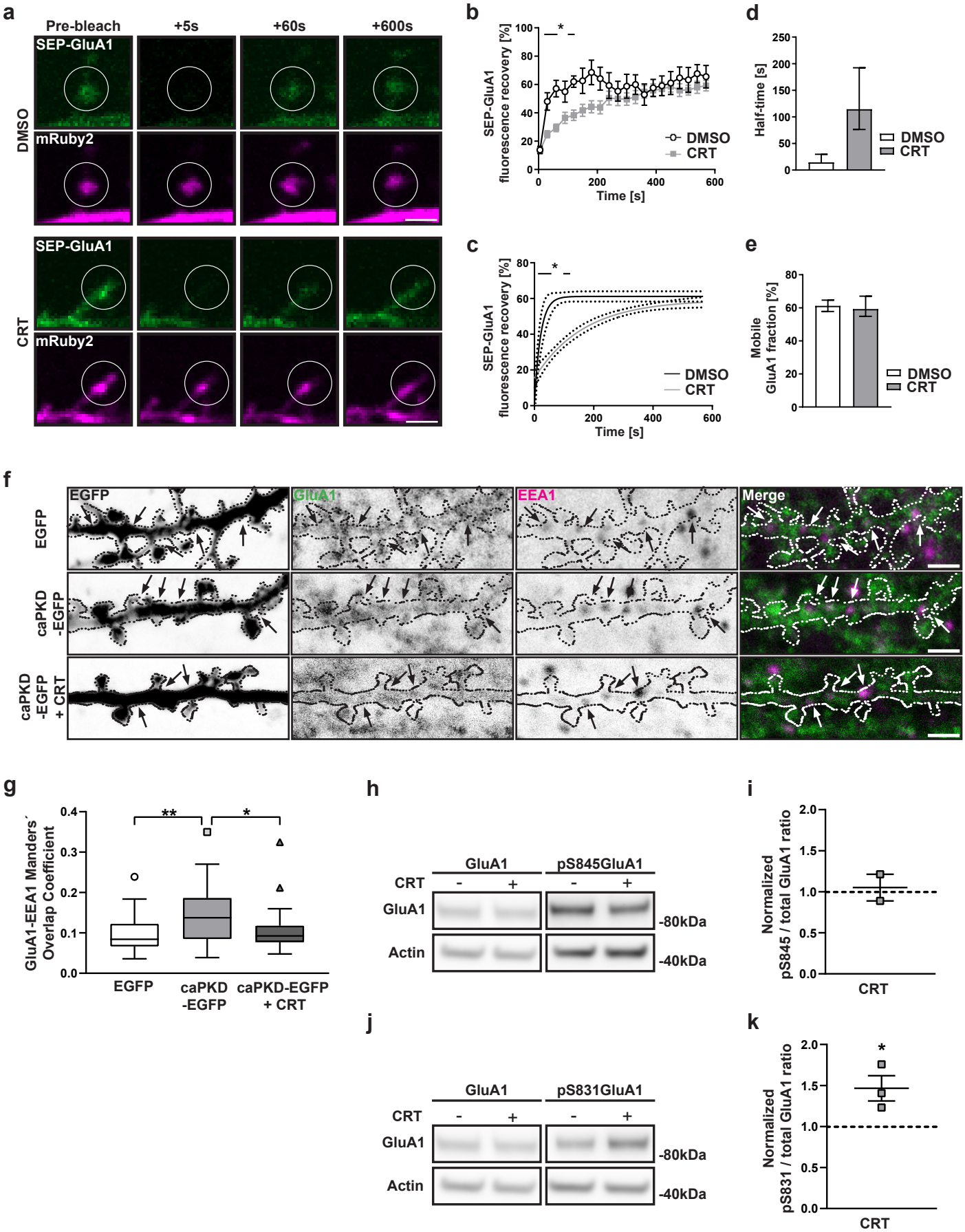
a
Pre-bleach
+5s
+60s
+600s
SEP-GluA1
mRuby2
DMSO
CRT
b
SEP-GluA1 fluorescence recovery [%]
Time [s]
DMSO
CRT
c
SEP-GluA1 fluorescence recovery [%]
Time [s]
DMSO
CRT
d
Half-time [s]
DMSO
CRT
e
Mobile GluA1 fraction [%]
DMSO
CRT
f
EGFP
GluA1
EEA1
Merge
EGFP
caPKD -EGFP
caPKD -EGFP + CRT
g
GluA1-EEA1 Manders´ Overlap Coefficient
EGFP
caPKD -EGFP
caPKD-EGFP + CRT
h
GluA1
pS845GluA1
CRT
GluA1
Actin
-80kDa
-40kDa
i
Normalized pS845 / total GluA1 ratio
CRT
j
GluA1
pS831GluA1
CRT
GluA1
Actin
-80kDa
-40kDa
k
Normalized pS831 / total GluA1 ratio
CRT

Figure 3

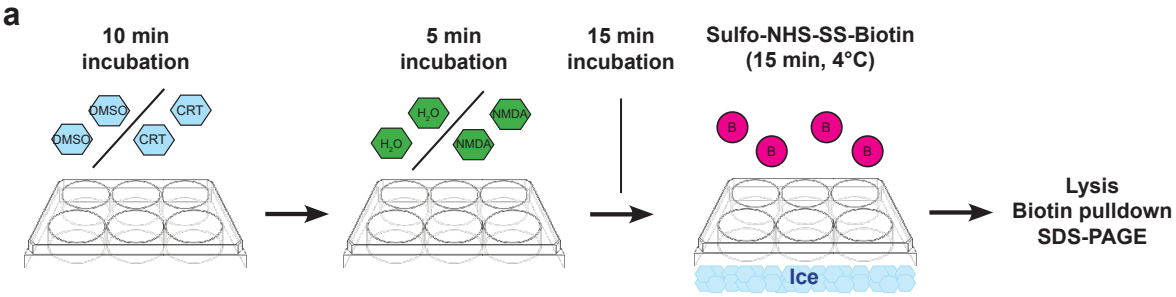
a
10 min incubation
5 min incubation
15 min incubation
Sulfo-NHS-SS-Biotin (15 min, 4°C)
DMSO
CRT
DMSO
CRT
H2O
NMDA
H2O
NMDA
B
B
B
B
Ice
Lysis
Biotin pulldown
SDS-PAGE

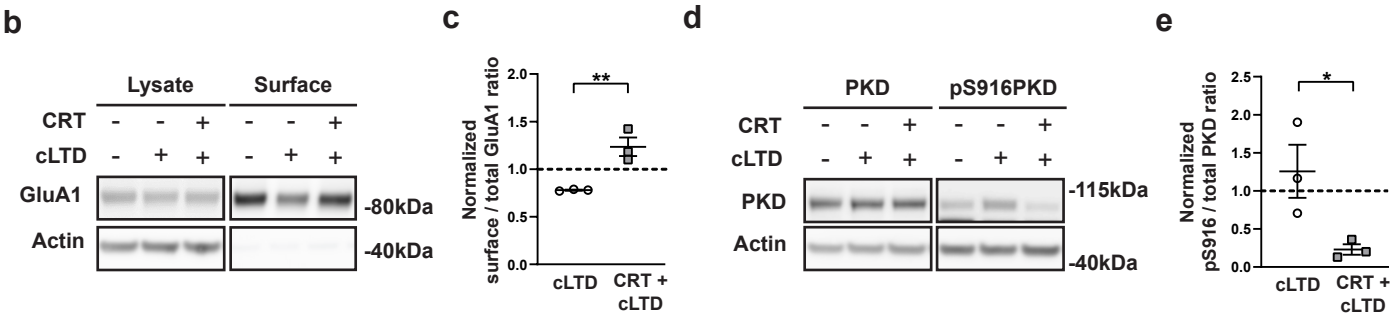
b
Lysate
Surface
CRT - - + - - +
cLTD - + + - + +
GluA1
Actin
-80kDa
-40kDa
c
Normalized surface / total GluA1 ratio
2.0
1.5
1.0
0.5
0.0
**
cLTD
CRT + cLTD
d
PKD
pS916PKD
CRT - - + - - +
cLTD - + + - + +
PKD
Actin
-115kDa
-40kDa
e
Normalized pS916 / total PKD ratio
2.5
2.0
1.5
1.0
0.5
0.0
*
cLTD
CRT + cLTD

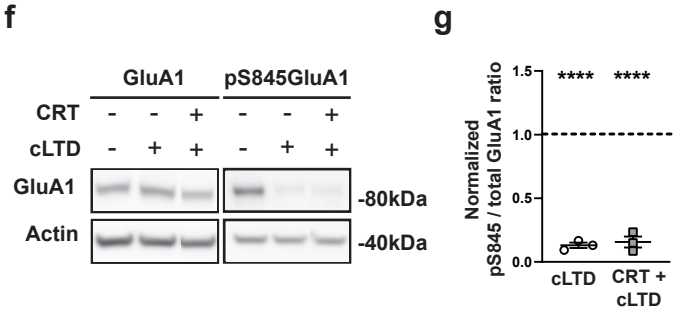
f
GluA1
pS845GluA1
CRT - - + - - +
cLTD - + + - + +
GluA1
Actin
-80kDa
-40kDa
g
Normalized pS845 / total GluA1 ratio
1.5
1.0
0.5
0.0
****
****
cLTD
CRT + cLTD

Figure 4

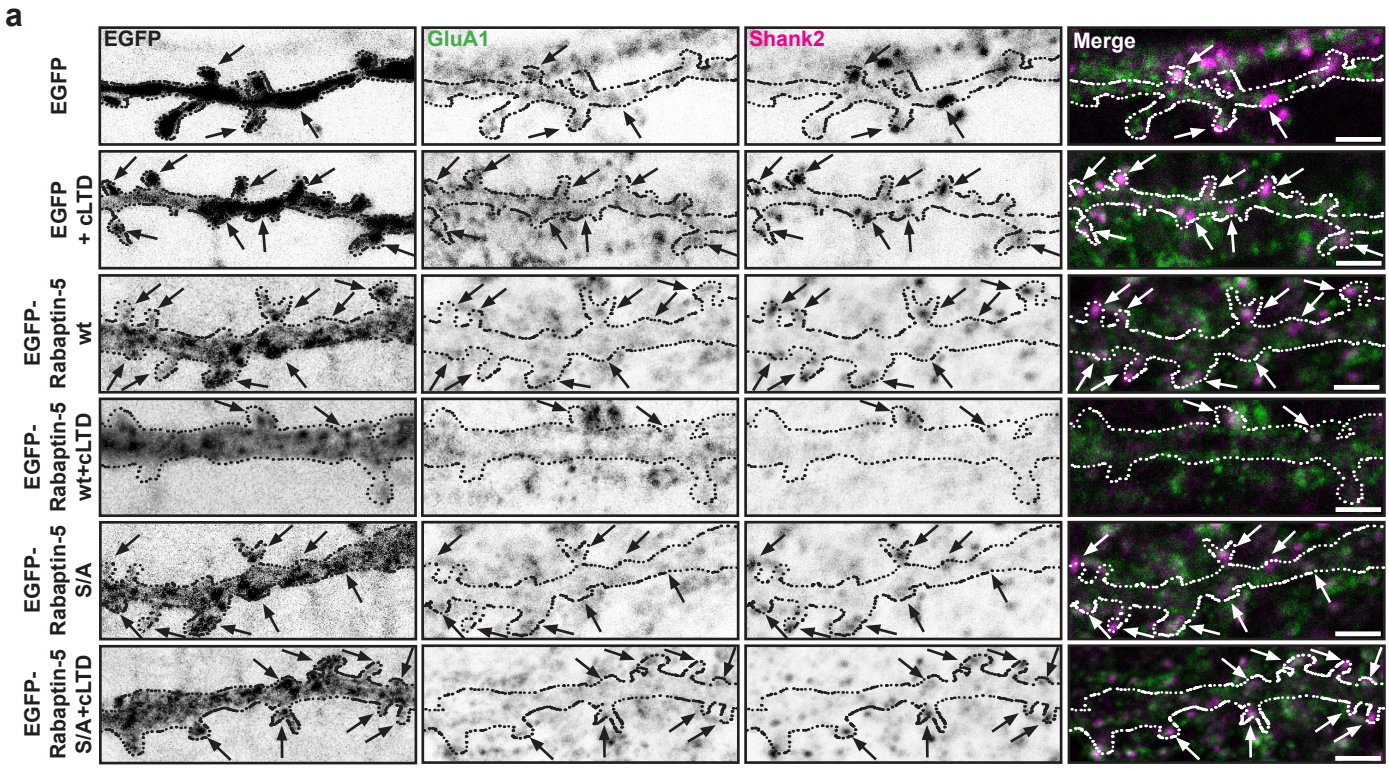
a
EGFP
GluA1
Shank2
Merge
EGFP
EGFP + cLTD
EGFP-Rabaptin-5 wt
EGFP-Rabaptin-5 wt+cLTD
EGFP-Rabaptin-5 S/A
EGFP-Rabaptin-5 S/A+cLTD

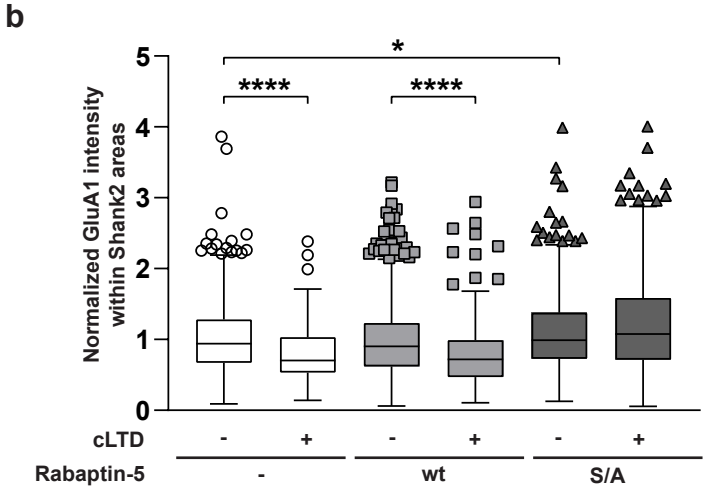
b
Normalized GluA1 intensity within Shank2 areas
0
1
2
3
4
5
*
****
****
cLTD
-
+
-
+
-
+
Rabaptin-5
-
wt
S/A

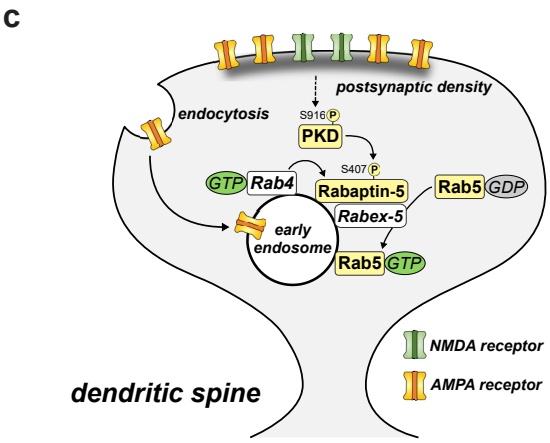
c
postsynaptic density
endocytosis
S916 P
PKD
S407 P
GTP Rab4
Rabaptin-5
Rab5 GDP
Rabex-5
early endosome
Rab5 GTP
NMDA receptor
AMPA receptor
dendritic spine
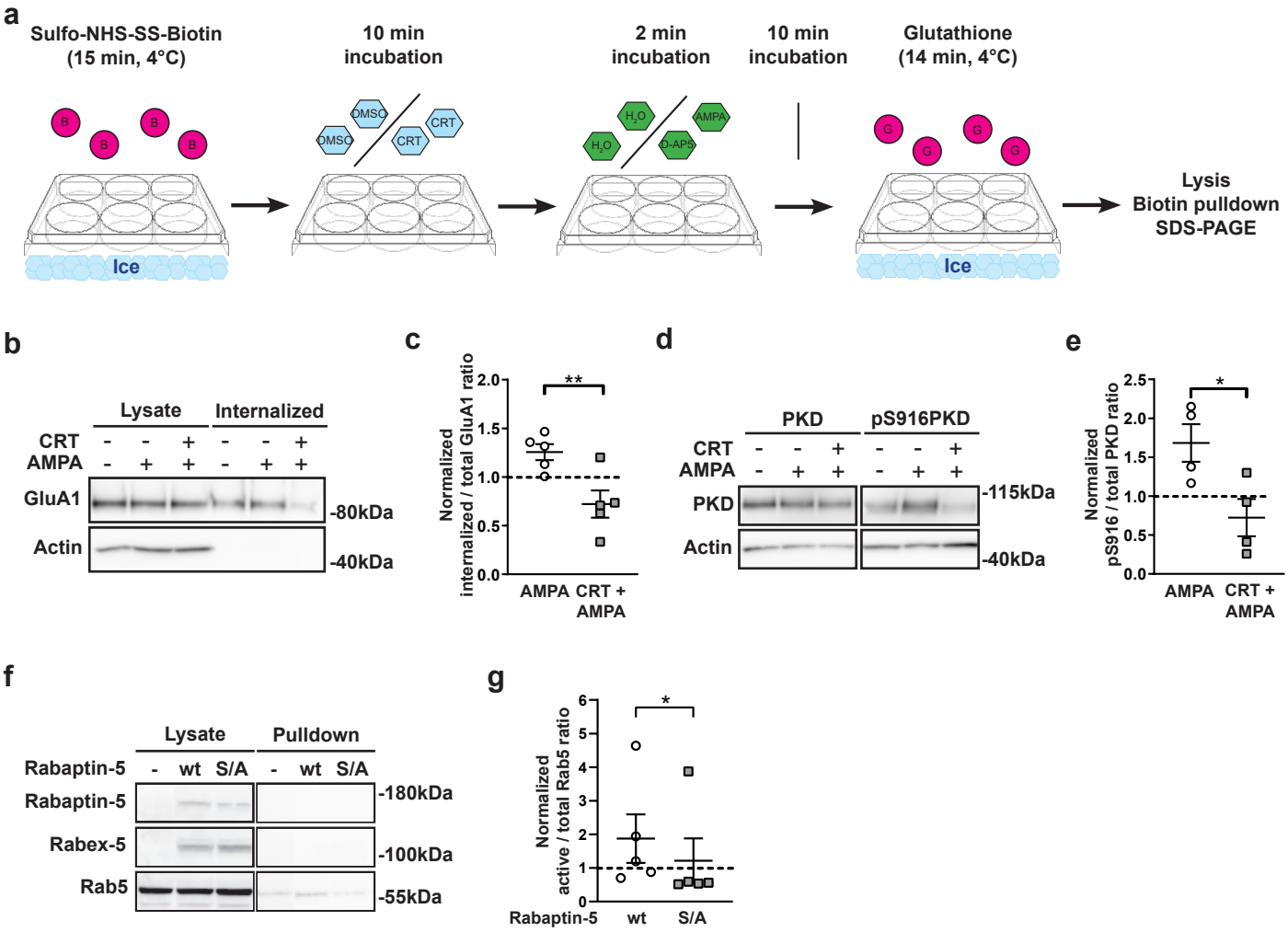
Supplementary figure 1